Carbohydrate Polymers 248 (2020) 116785

Contents lists available at ScienceDirect

Carbohydrate Polymers

journal homepage: www.elsevier.com/locate/carbpol

Inhibition of glucuronomannan hexamer on the proliferation of lung cancer through binding with immunoglobulin G

Weihua Jin[a,b], Xinyue He[a], Jiachen Zhu[a], Qiufu Fang[a], Bin Wei[c], Jiadong Sun[d,e], Wenjing Zhang[f], Zhongshan Zhang[g], Fuming Zhang[b], Robert J. Linhardt[b,h], Hong Wang[c,*], Weihong Zhong[a,*]

[a] College of Biotechnology and Bioengineering, Zhejiang University of Technology, Hangzhou, 310014, China
[b] Department of Chemical and Biological Engineering, Center for Biotechnology and Interdisciplinary Studies, Rensselaer Polytechnic Institute, Troy, NY, 12180, USA
[c] Collaborative Innovation Center of Yangtze River Delta Region Green Pharmaceuticals & College of Pharmaceutical Sciences, Zhejiang University of Technology, Hangzhou, 310014, China
[d] Department of Biomedical and Pharmaceutical Sciences, College of Pharmacy, University of Rhode Island, Kingston, RI, 02881, USA
[e] Laboratory of Bioorganic Chemistry, National Institute of Diabetes and Digestive and Kidney Diseases (NIDDK), National Institutes of Health, Bethesda, MD, 20878, USA
[f] Department of Endocrinology, Sir Run Run Shaw Hospital, Zhejiang University School of Medicine, Hangzhou, 310016, China
[g] Key Laboratory of Vector Biology and Pathogen Control of Zhejiang Province, Huzhou University, Huzhou, 313000, China
[h] Department of Biological Science, Departments of Chemistry and Chemical Biology and Biomedical Engineering, Center for Biotechnology and Interdisciplinary Studies, Rensselaer Polytechnic Institute, Troy, NY, 12180, USA

ARTICLE INFO

Keywords:
Glucuronomannan
Anti-lung cancer activity
SPR
Fucoidan
Proteomics

ABSTRACT

The anti-lung cancer activity of oligosaccharides derived from glucuronomannan was investigated. The inhibition of A549 cell proliferation by glucuronomannan (Gn) and its oligomers (dimer (G2), tetramer (G4) and hexamer (G6)) were concentration dependent. *In vivo* activities on the A549-derived tumor xenografts showed the tumor inhibition of G2, G4 and G6 were 17 %, 40 % and 46 %, respectively. Organ coefficients in nude mice showed an increase in the kidney with G4, the brain with G6, and the spleen with G6. An advanced tandem mass tag labeled proteomics approach was performed. A significant differential expression was found in 59 out of the 4371 proteins, which involved the immune system. Surface plasmon resonance (SPR) studies revealed G6 was strongly bound to immunoglobulin G. This suggests that glucuronomannan hexamer inhibits the proliferation of lung cancer through its binding to immunoglobulin.

1. Introduction

Glucuronomannan (Gn) is composed of alternating 1, 4-linked β-D-GlcAp residues and 1, 2-linked α-D-Manp residues (Jin, Wang, Ren, Song, & Zhang, 2012; Jin, Ren, Liu, Zhang, & Zhong, 2018; Wang et al., 2012; Wu et al., 2015). Gn can be prepared by degradation of polysaccharides (fucoidan) from brown algae. There are many reviews on the activities of fucoidan (Berteau & Mulloy, 2003; Cumashi et al., 2007; Deniaud-Bouet, Hardouin, Potin, Kloareg, & Herve, 2017; Fitton, 2011; Fitton, Stringer, & Karpiniec, 2015; Garcia-Vaquero, Rajauria, O'Doherty, & Sweeney, 2017; Hsu & Hwang, 2019; Kusaykin et al., 2008; Lee et al., 2017; Li, Lu, Wei, & Zhao, 2008; Luthuli et al., 2019; Pomin, 2010; Pomin & Mour˜ao, 2008; Sanjeewa, Lee, Kim, & Jeon, 2017; Usov & Bilan, 2009; Wijesinghe & Jeon, 2012; Wu et al., 2016; Zaporozhets & Besednova, 2016). However, to our knowledge, there have been no reports on the biological activities of Gn or its oligomers, except for the antioxidant activities of sulfated glucuronomannan oligosaccharides (Jin et al., 2018).

Oligosaccharides have many advantages over polysaccharides, including a controlled structure facilitating quality control and the ability to pass through biological barriers. Today, there are many types of oligosaccharide therapeutic agents under investigation including heparin-oligosaccharides (Liu & Linhardt, 2014), chitosan (Muanprasat & Chatsudthipong, 2017; Yuan et al., 2019), human milk oligosaccharides (Ackerman et al., 2018; Ray et al., 2019), fructooligossaccharides (Gremski et al., 2019), fucosylated chondroitin sulfate oligomers (Yan et al., 2019), neoagaro-oligosaccharides (Lin et al., 2019), alginate oligosaccharides (Lang, Zhao, Liu, & Yu, 2014), pectic oligosaccharides (Wilkowska et al., 2019) and manno-oligosaccharide (Li, Yi, Liu, Yan, & Jiang, 2018).

Oligosaccharides play critical roles in a wide range of biological processes (Feng et al., 2015; Kim et al., 2017; Yadav et al., 2015; Zhang et al., 2013; Zhang, Lee, & Linhardt, 2015; Zhang, Zheng et al., 2019; Zhang, Yan et al., 2019; Zhao et al., 2017). Fucosylated chondroitin

* Corresponding authors.
E-mail addresses: hongw@zjut.edu.cn (H. Wang), whzhong@zjut.edu.cn (W. Zhong).

https://doi.org/10.1016/j.carbpol.2020.116785
Received 18 March 2020; Received in revised form 15 July 2020; Accepted 16 July 2020
Available online 21 July 2020

sulfate oligosaccharides, for example, display potent anticoagulant activities (Yan et al., 2019). Neoagaro-oligosaccharides are beneficial in controlling the level of blood glucose and ameliorating the damage of the liver and pancreatic islets (Lin et al., 2019). Pectin-derived oligosaccharides are important as prebiotics for human and animals by stimulating bowel colonization with lactic acid bacteria and inhibiting the development of infections caused by pathogens (Wilkowska et al., 2019). Human milk oligosaccharides possess antimicrobial and antibiofilm activities (Ackerman et al., 2018).

Many researchers have shown that the immune system can clear or suppress the majority of carcinomas and immunomodulation exhibits a vital role in the protection against tumor development (Agha-Mohammadi & Lotze, 2000; Ehrrlich, 1999; Khalil, Smith, Brentjens, & Wolchok, 2016; Locy et al., 2018; Matsushita & Kawaguchi, 2018). Many oligosaccharides and derivatives showed immunomodulatory effects. It has been reported that feruloylated oligosaccharides display immunomodulatory effects against mouse colitis through the immune balance of Th17 and Treg cells (Xia et al., 2019). HMO-7, one of neutral human milk oligosaccharides (HMO), showed immunomodulatory effects by producing inflammatory mediators and cytokines including nitric oxide, PGE2, ROS, tumor necrosis factor α (TNF-α), and some certain interleukins (Zhang, Zheng et al., 2019; Zhang, Yan et al., 2019). In addition, HMO exerts an anti-inflammatory effect by reducing the platelet-neutrophil complex formation, inhibiting the leukocyte rolling and adhesion to endothelial cells, influencing cytokine production and developing the immune system, potentially leading to a more balanced Th1/Th2 response (Ray et al., 2019). Chitooligosaccharides show immunostimulatory, immunoregulatory and anti-inflammatory properties through their interaction with membrane receptors on the macrophage surface (dependent on toll-like receptor 4), boosting the expression of key gene of nuclear factor kappa B and triggering the protein phosphorylation (Guan et al., 2019). Pretreatment with the oligosaccharides from κ- or ι-carrageenan displayed the anti-inflammatory activity by decreasing TNF-α (Ai et al., 2018). Galactooligosaccharides derived from lactulose with *Saccharomyces cerevisiae* can bind immune cell receptor Dectin-2 (Young et al., 2019).

So far, there have been only limited studies of the structure-activity relationship between the degree of polymerization (DP) and the anti-lung cancer activity of Gn and its oligomers. The hypothesis in the current study is that Gn and its derivatives could exhibited the anti-lung cancer activity through the immune system. Our aim is to probe the effects of DP on the anti-lung cancer activity of Gn and its oligomers. In addition, proteomics and surface plasmon resonance (SPR) competition studies have been performed to elucidate the mechanism of the anti-lung cancer activity.

2. Materials and methods

2.1. Characterization, preparation and purification of glucuronomannan and its oligomers

Gn oligomers (G2, G4 and G6, disaccharide through hexasaccharide) were prepared in our laboratory by the methods described in our previous study (Jin et al., 2012, 2018). In brief, crude polysaccharide from *Sargassum thunbergii* was degraded with reflux (110 °C) in 0.5 M sulfuric acid (60 mg/mL) for 5 h and then neutralized, centrifuged and concentrated. The concentrated sample was fractionated using an activated carbon column (2.6 cm × 30 cm, activated charcoal was purchased from Sigma-Aldrich (Cat # 31616)) with water (Y1) and 75 % ethanol (Y2). The eluent Y2 was combined, concentrated and freeze-dried. Y2 (0.5 g) was separated on a Bio-Gel P-4 Gel column (Extra Fine, 2.6 cm × 100 cm) and then eluted with 0.5 M NH_4HCO_3 at a flow rate of 0.15 mL/min. Oligomers (G2, G4 and G6) were collected and lyophilized.

Gn low molecular weight (7.0 kDa) polysaccharide was prepared from the crude polysaccharide. It was refluxed (110 °C) in 0.5 M sulfuric acid for 5 h and then neutralized, centrifuged and concentrated. Anion exchange chromatography on a DEAE-Bio Gel agarose FF Gel (6 cm × 40 cm) was performed with elution with 0.2 M NaCl, 0.5 M NaCl and 2 M NaCl. The resulting polysaccharide fractions were desalted using Sephadex G10 chromatography (3.5 cm × 30 cm). Finally, the desalted 2 M NaCl fraction was lyophilized to obtain Gn.

The molecular weight of Gn was measured by gel permeation chromatography (GPC)-high performance liquid chromatography (HPLC) on TSK G3000 PWxl column (7 μm 7.8 × 300 mm) with elution in 0.05 M Na_2SO_4 at a flow rate of 0.5 mL/min at 40 °C using refractive index detection. Different molecular weight dextrans (2.5, 4.6, 7.1, 21.4, 41.1 and 133.8 k Da) from the National Institute for the Control of Pharmaceutical and Biological Products (Beijing, China), were used as molecular weight standards.

2.2. Anti-lung cancer activity

Anti-lung cancer activities using human lung cancer A549 cells were next determined. Cell viability was measured using 3-(4, 5-dimethylthiazol-2-yl)-2, 5-diphenyl tetrazolium (MTT) assay. Briefly, cells were cultured in RPMI 1640 medium containing 10 % fetal bovine serum and penicillin-streptomycin (100 units/ mL) in an atmosphere of 5% CO_2 at 37 °C. The cells (100 μL) were then seeded in a 96-well plate at a density of 1×10^4 cells/well and cultured for 24 h. The cells were divided into three groups: (1) a blank group only containing medium; (2) a control group in which cells were added; and (3) an experimental group containing cells and different concentrations of Gn cultivated in medium. After removal of the media, 10 μL of MTT (5 mg/mL) was added to each well. After 4 h of incubation, the supernatants were removed, and dimethylsulfoxide (DMSO) (100 μL) was added. The absorbance was measured and inhibition was determined using the following equation: Cell Inhibition (%) = (Ac − A1)/(Ac − A0) × 100, where A0 was the absorbance of the blank, A1 was the absorbance in the presence of sample, and Ac was the absorbance of the control.

2.3. Xenograft tumor model

Four-week-old male BALB/c-nu nude mice were purchased from Shanghai Sipu-bikai Experimental Animal Co., LTD (Shanghai, China). All studies in mice were approved (NO. 11/2017) by the Animal Ethics Committee of Zhejiang University of Technology Animal Center in accordance with the animal care and use guidelines. Tumors were established by giving a *subcutaneous* injection of 2.5×10^6 (0.2 mL) A549 cells into the right flank of mice. Xenograft mice were administrated *i.p.* with G2, G4, G6 and Gn doses at 100 mg/kg (0.2 mL) every day, while equal volume of normal saline was injected as a control. Drug-treatment was initiated after tumors were palpable and lasted for approximately 11 days. Body weight and tumor volumes were measured every two days using a balance and with a vernier caliper. The tumor volumes were calculated from the formula: V = ½ × length × width^2 and the relative tumor volumes (RTV) were calculated with the formula: Vn/V0 (Vn represents the tumor volume at the "n" day after administration and V0 corresponds to the tumor volume before administration). After treatment, the mice were euthanized to excise tumors. The tumor inhibition was calculated based on the following formula: (the mean tumor weight of control group - the mean tumor weight of treated group)/ the mean tumor weight of control group × 100. The organ coefficients of nude mice were calculated from the formula: organ weight × 1000 / body weight. The flow chart of A549 cells xenograft tumor model is shown in Fig. S1.

2.4. Protein analysis

The tumors in the G6 group and control group were ground and added with four-volumes of lysis buffer, containing 8 M urea, 1% protease inhibitor and 2 mM EDTA. Ultrasonic lysis was then performed

Table 1
The chemical shifts of G2, G4, G6 and Gn.

Samples	Residues	C1	C2	C3	C4	C5	C6	H1	H2	H3	H4	H5	H6
G2	→2)-α-D-Manp-OH	92.5	78.8	69.8	67.3	72.7	60.8	5.15	3.95	3.75	3.58	3.58	3.58 – 3.69
	β-D-GlcAp-(1→	102.0	72.9	75.6	72.1	76.1	176.1	4.38	3.24	3.39	3.69	3.69	–
G4	→2)-α-D-Manp-OH	92.4	78.6	69.8	67.4	72.7	60.9	5.14	3.91	3.73	3.55	3.58	3.63 – 3.69
	→4)-β-D-GlcAp-(1→	101.9	73.0	76.7	77.2	76.4	175.3	4.37	3.22	3.55	3.63	3.66	–
	→2)-α-D-Manp-(1→	98.8	77.9	69.9	66.8	72.9	60.4	5.28	4.05	3.71	3.58	3.58	3.63 – 3.69
	β-D-GlcAp-(1→	101.8	73.1	75.6	72.2	76.2	176.2	4.33	3.27	3.38	3.63	3.66	–
G6	→2)-α-D-Manp-OH	92.4	78.6	69.9	67.4	72.9	60.9	5.14	3.91	3.68	3.53	3.58	3.63 – 3.68
	→4)-β-D-GlcAp-(1→	101.9	73.0	76.4	77.2	76.7	175.4	4.36	3.26	3.53	3.63	3.66	–
	→2)-α-D-Manp-(1→	98.8	77.8	69.9	66.8	73.0	60.4	5.27	4.02	3.68	3.58	3.58	3.63 – 3.68
	→4)-β-D-GlcAp-(1→	101.7	73.0	76.4	77.2	76.7	175.4	4.32	3.26	3.53	3.63	3.66	–
	→2)-α-D-Manp-(1→	98.8	77.9	69.9	66.8	73.0	60.4	5.27	4.05	3.68	3.58	3.58	3.63-3.68
	β-D-GlcAp-(1→	101.7	73.0	75.6	72.2	76.7	176.2	4.32	3.26	3.37	3.62	3.66	–
Gn	→2)-α-D-Manp-OH	–	78.6	69.8	67.4	72.7	–	5.14	3.90	3.73	3.52	3.58	3.63 – 3.68
	→4)-β-D-GlcAp-(1→	102.0	73.0	76.8	77.1	76.4	175.4	4.32	3.25	3.52	3.63	3.66	–
	→2)-α-D-Manp-(1→	98.8	77.8	69.9	66.8	72.9	60.4	5.27	4.02	3.71	3.58	3.58	3.63 – 3.68
	β-D-GlcAp-(1→	101.8	73.1	75.6	72.2	76.4	–	4.32	3.27	3.39	3.63	3.66	–

and samples were centrifuged to obtain soluble proteins. The protein concentration was determined using a BCA kit. Proteins were then digested by trypsin and tandem mass tag (TMT) labeled according to the manufacturer's protocol. Briefly, one unit of TMT reagent were thawed and reconstituted in acetonitrile. The peptide mixtures were then incubated for 2 h at room temperature and pooled, desalted and dried by vacuum centrifugation. The tryptic peptides were fractionated into fractions by high pH reversed-phase HPLC using Agilent 300 Extend C18 column (5 μm particles, 4.6 mm ID, 250 mm length). Briefly, peptides were first separated into 60 fractions with a gradient of 8%–32% acetonitrile (pH 9.0) over 60 min. Peptides were combined into 18 fractions and dried by vacuum centrifugation. The peptides were subjected to NSI source followed by tandem mass spectrometry (MS/MS) in Q ExactiveTM Plus (Thermo) coupled online to the UPLC. The electrospray voltage applied was 2.0 kV. The *m/z* scan range was 350–1800 for full scan, and intact peptides were detected in the Orbitrap at a resolution of 70,000. Peptides were selected for MS/MS using NCE setting as 28 and the fragments were detected in the Orbitrap at a resolution of 17,500. A data-dependent procedure that alternated between one MS scan followed by 20 MS/MS scans with 15.0 s dynamic exclusion. Fixed first mass was set as 100 *m/z*.

2.5. Database search and bioinformatics

The resulting MS/MS data were processed using Maxquant search engine (v.1.5.2.8). Tandem mass spectra were searched against SwissProt Mouse database concatenated with reverse decoy database. GO Annotation: Gene Ontology (GO) annotation proteome was derived from the UniProt-GOA database (www. http://www.ebi.ac.uk/GOA/). Domain Annotation: Identified proteins domain functional description was annotated by InterProScan (a sequence analysis application) based on protein sequence alignment method, and the InterPro (http://www.ebi.ac.uk/interpro/) domain database was used. KEGG Pathway Annotation: Kyoto Encyclopedia of Genes and Genomes (KEGG) database was used to annotate protein pathway. Subcellular Localization: We used Wolfpsort a subcellular localization predication soft to predict subcellular localization. Wolfpsort is an updated version of PSORT/PSORT II for the prediction of eukaryotic sequences. For prokaryotic species, subcellular localization prediction soft CELLO was used. Enrichment of Gene Ontology analysis: Proteins were classified by GO annotation into three categories: biological process, cellular compartment and molecular function. For each category, a two-tailed Fisher's exact test was employed to test the enrichment of the differentially expressed protein against all identified proteins. The GO with a corrected p-value < 0.05 is considered significant. Enrichment of protein domain analysis: For each category proteins, InterPro (a resource that provides functional analysis of protein sequences by classifying them into families and predicting the presence of domains and important sites) database was researched and a two-tailed Fisher's exact test was employed to test the enrichment of the differentially expressed protein against all identified proteins. Protein domains with a p-value < 0.05 were considered significant.

2.6. SPR solution competition study between glucuronomannan and its oligomers binding to immunoglobulin G (IgG)

Solution competition SPR measurements were performed on a BIAcore 3000 (GE Healthcare, Uppsala, Sweden). Heparin chip was prepared according to the previous studies (Zhang, Zheng et al., 2019; Zhang, Yan et al., 2019). To measure the inhibition of glucuronomannan and its oligomers on immunoglobulin G (IgG) binding to heparin surface, IgG was pre-mixed with different concentrations of glucuronomannan and its oligomers and injected over the heparin chip at 30 μL/min. After each run, a dissociation period and regeneration with 2 M NaCl was performed.

2.7. Statistics analysis

All data are shown as the mean ± standard deviation (SD). Significant differences between experimental groups were determined by one-way ANOVA, and differences were considered as statistically significant if $p \leq 0.05$. All calculations were performed using SPSS 16.0 statistical Software.

3. Results

3.1. Characterization of glucuronomannan and its oligomers

The yields based on fraction Y2 of glucuronomannan oligomers (G2, G4 and G6) were 40.1 %, 20.4 % and 9.3 %, respectively. The ^{1}H and DEPTQ (^{13}C) NMR spectra of G2 to G6 were showed in Figs. S2–S4. The GPC-HPLC chromatogram of glucuronomannan low molecular weight polysaccharide Gn, presented in Fig. S5, shows a molecular weight of 7.0 kDa. Moreover, the ^{1}H and DEPTQ (^{13}C) and HSQC spectrum of Gn was displayed in Figs. S6 and S7. A summary of chemical shifts of G2, G4, G6 and Gn is presented in Table 1.

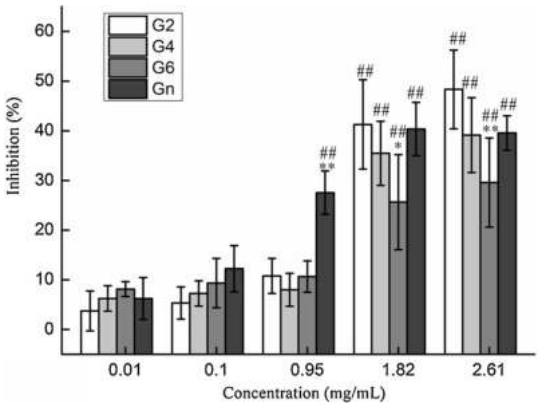

Fig. 1. The proliferation inhibition of G2, G4 and G6 and Gn on A549 cells. Cells were cultured in 96-well plate and treated with different concentrations of G2, G4, G6 and Gn (0.01–2.61 mg/mL) for 24 h. The cell viability was analyzed by MTT assay. Data are presented as means ± SD of three independent experiments (n = 3). Significant difference from the G2 group at the same concentration was designated as *P ≤ 0.05 and **P ≤ 0.01; Significant difference from the 0.01 mg/mL group of the same sample was designated as #P ≤ 0.05 and ##P ≤ 0.01.

3.2. The inhibition of glucuronomannan and its oligomers on the proliferation of A549 cells

A549 cells were exposed to increasing concentrations of G2, G4, G6 and Gn for 24 h to evaluate the proliferation inhibitions by G2, G4, G6 and Gn, and cellular inhibition was determined (Fig. 1). There was no significant difference among the samples at concentrations below 0.95 mg/mL, except Gn at the concentration of 0.95 mg/mL. However, G6 showed the lowest activity and other samples showed no significant difference at concentrations of 1.82 and 2.61 mg/mL. In summary, the results obtained were too complicated to draw firm conclusion on the impact of DP on anti-proliferative activity.

3.3. Glucuronomannan and oligomers attenuated A549 xenograft tumor growth in vivo

The medicinal effects of Gn and its oligomers in BALB/c-nu mice were next determined. The tumor inhibition rates of G2, G4, G6 and Gn were 17 %, 40 %, 46 % and −10 %, respectively, suggesting that G4 and G6 could significantly inhibit the growth of A549 tumors (Figs. 2A, B and S8). The relative tumor volume (RTV) of each group is shown in Fig. 2C. G6 significantly inhibited the tumor growth compared with the control. The inhibition calculated by RTV was 55 %, which was higher than the tumor inhibition (46 %). In addition, the body weights (Fig. 2D) were relatively stable. These data suggest that Gn oligomers G4 and G6 were potent and well tolerated by test animals. Compared with the control group, the organ coefficients of heart, liver, lungs, kidney and brain showed no apparent differences, except for the organ coefficients of G4 treated kidney, G6 treated brain and G6 treated spleen (Table 2). The kidney coefficient of G4 treated animals and the brain coefficient of G6 treated animals were larger than those of the control group. Compared with the spleen coefficient in the control group, it is interesting to note that the spleen coefficients of the G6 treated animals were increased significantly while the spleen coefficient of G4 treated animals showed an insignificant increase. The increase of spleen coefficient suggested the anti-tumor activity involved cellular and humoral immunity (Fan et al., 2018; Mebius & Kraal, 2005). Therefore, we conclude that G6 might represent a good candidate for use in the treatment of lung cancer.

3.4. Proteome overview and protein annotation

We next investigated the global protein expression profiles of the tumors at 21 days of treatment with G6 at the proteome level using an advanced TMT labeled proteomics approach to elucidate the mechanism of anti-lung cancer activity. By searching against the SwissProt Mouse database, 5152 proteins were identified from a total of 289847 spectra, 29995 peptides, and 28696 unique peptides in the proteomic analysis. Out of the 4371 proteins 59 showed significantly differential expression under p-value < 0.05 and fold-change > 1.5. All of the proteins identified were annotated using the Kyoto Encyclopedia of Genes and Genomes (KEGG) and National Center for Biotechnology Information non-redundant protein sequences (NCBInr) databases.

3.5. Gene Ontology (GO) analysis of differentially expressed proteins

GO was used to classify the function of the differentially expressed tumors proteins. There were 59 differentially expressed proteins, containing 42 upregulated proteins and 17 downregulated proteins. They were classified into three main categories: biological process, cellular component, and molecular function.

Fourteen secondary categories exist in the biological process of upregulated proteins. Among these categories, single-organism process, cellular process, biological regulation, response to stimulus, metabolic process, multicellular organismal process, immune system process, localization, cellular component organization or biogenesis, developmental process, multi-organism process, signaling, locomotion and others accounted for 14 %, 12 %, 11 %, 10 %, 9 %, 8 %, 7 %, 7 %, 5 %, 5 %, 5 %, 4 %, 2 % and 1 %, respectively (Fig. 3). Cellular component had seven secondary categories, among which, cellular was the largest categories, representing 26 %, followed by 19 % extracellular region, 17 % organelle, 14 % membrane and macromolecular complex, 9% supramolecular complex and 1% other. Binding represented 63 % of the molecular function, followed by 13 % catalytic activity, 7% structural molecule activity, 5% molecular function regulator. Moreover, the compositions of secondary categories in the three main categories for downregulated proteins (Fig. 3) were similar to those of upregulated proteins in general, except for some slight changes. However, the percentages of single-organism process, immune system process, localization, extracellular region, organelle, macromolecular complex, supramolecular complex, cell junction, membrane-enclosed lumen, binding, structural molecule activity, molecular function regulator, molecular transducer activity and signal transducer activity were changed more than or equal to three percent.

For upregulated proteins, fourteen other (from fourth to ninth) categories (Fig. 4) are present in the biological process, eight other (from secondary to ninth) categories are present in the cellular component and four other (from third to fifth) categories are present in the molecular function. For downregulated proteins, ten other (from fifth to ninth) categories (Fig. 4) are present in the biological process; two other (from fourth to fifth) categories are present in the cellular component. The antigen binding, GO secondary category, was the most significantly enriched in the upregulated proteins, while the positive regulation of T cell activation was the most significantly enriched in the downregulated proteins. Thus, we conclude that the most differentially expressed proteins were involved in the immune system.

3.6. Subcellular structure localization of differentially expressed proteins

The subcellular structure localizations of differentially expressed proteins are predicted and classified by using statistics and Wolfpsort software. The upregulated proteins were in the cytoplasm, extracellular, nucleus, mitochondria, endoplasmic reticulum, cytoplasm, nucleus and plasma membrane accounting for 32 %, 27 %, 19 %, 10 %, 5 %, 5 % and 2 %, respectively (Fig. 5). The downregulated proteins were in the nucleus, plasma membrane, extracellular, cytoplasm and

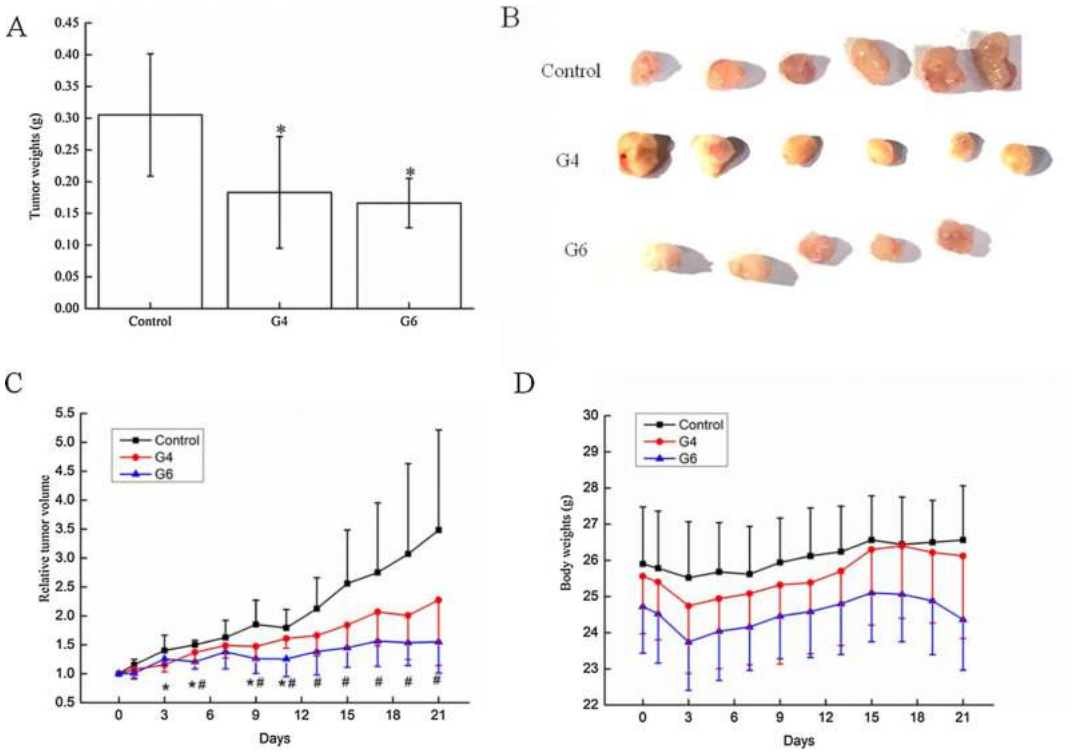

Fig. 2. Attenuation of A549 cell xenograft tumor growth in BALB/c-nu mice by oligomers (G4 and G6). (**A**) The tumor weight of each group, * $p < 0.05$ *versus* control. (B) Representative images of the A549 xenograft tumors from each group at day 21. Oligomers (100 mg/kg/d, intraperitoneal injection) were used for treatment groups. Control groups were treated with the corresponding solvents the same as treatment groups. (**C**) The relative tumor volume of each group; the relative tumor volume of G4, * $p < 0.05$ *versus* Control; The relative tumor volume of G6, # $p < 0.05$ *versus* Control; (**D**) The body weight of each group. Control group (n = 6), G4 group (n = 6) and G6 group (n = 5).

Table 2
Organ coefficients of nude mice.

Organ	Control	G4	G6
Heart	6.3 ± 1.0	6.3 ± 0.2	6.3 ± 0.5
Liver	56.9 ± 3.8	59.3 ± 6.3	58.0 ± 3.7
Spleen	3.1 ± 0.4	3.8 ± 0.5	4.5 ± 0.5**
Lungs	5.8 ± 0.4	5.4 ± 0.6	5.6 ± 1.2
Kidney	16.3 ± 1.4	19.6 ± 3.7*	17.2 ± 1.4
Brain	14.5 ± 3.1	16.1 ± 0.7	17.0 ± 0.7*

Notes: *$p < 0.05$, ** $p < 0.01$ *versus* Control.

cytoplasm, nucleus accounting for 29 %, 23 %, 18 %, 18 % and 12 %, respectively. Thus, the differentially expressed proteins were primarily nuclear, extracellular and cytoplasmic.

3.7. Protein domains enrichment analysis of up and down regulated proteins

The protein domain enrichment analysis (Fig. 6) indicated that many of the upregulated proteins contained the following domains: immunoglobulin-like domain, immunoglobulin-like fold, immunoglobulin V-set domain, immunoglobulin subtype, immunoglobulin C1-set, EF-hand domain pair and EF-hand domain. In contrast, the downregulated proteins contain no observed domains.

3.8. SPR solution competition study between glucuronomannan and its oligomers and immunoglobulin G (IgG)

For IgG very strong inhibitory activities (> 80 %) were observed at concentrations of 0.10, 0.50 and 2.50 mg/mL for Gn. Strong inhibitory activities (> 60 %) were observed at concentrations of 1.0 μM of Gn, 0.5 and 2.5 mg/mL of G6, and 2.5 mg/mL of G4 (Fig. 7). Modest inhibitory activities (> 40 %) were observed at concentration of 0.5 mg/mL of G4. Other interactions were weak (lower than 40 % and higher than 20 %). No concentration dependence was observed for any of the samples.

4. Discussion

Gn and its oligomers (G2, G4 and G6) were prepared. The results on the proliferation on A549 cells *in vitro* showed that G2, G4, G6 and Gn exhibited only 3 %–10 % at concentrations lower than 0.95 mg/mL, except Gn, which showed 28 % inhibition at a concentration of 0.95 mg/mL. The inhibitions of G6 were 26 % and 30 %, at concentrations of 1.82 and 2.61 mg/mL, respectively, were the lowest inhibition among all the samples. The inhibitions of G2, G4 and Gn, fluctuated between 35 % and 48 % at concentrations of 1.82 and 2.61 mg/mL, respectively, and showed no significant differences. However, the A549 cell xenograft tumor model in BALB/c-nu mice indicated that G6 showed the strongest inhibition of about 46 %, followed by G4 (40 % inhibition), and G2 and Gn showed weak inhibition *in vivo*. The body weights of treated animals were relatively stable. The organ coefficients of nude mice indicated that the spleen coefficient of G6 was larger than the control group. Previous studies (Chen et al., 2012) suggest that the spleen index reflects the immune function and immunopotentiator could increase the weights of spleen, which is consistent with the results of proteomics analysis. It was shown that the most differentially expressed proteins were involved in the immune system. Further studies on the interaction between immunoglobulin G and Gn oligomers were undertaken using surface plasmon resonance. It was shown Gn had the strongest inhibitory activities. G6 showed the

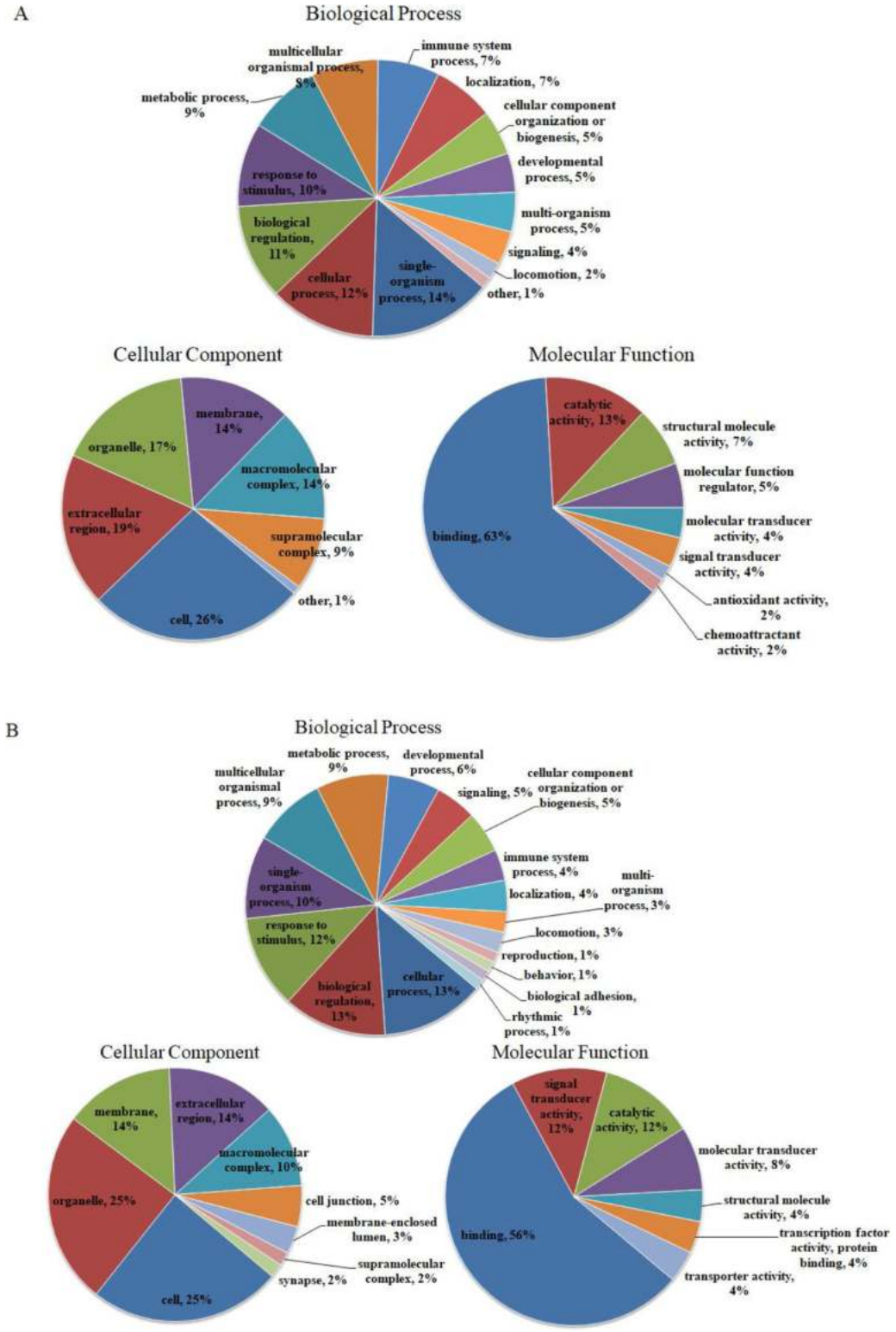

Fig. 3. GO secondary categories assigned to the significantly up (A) and down (B) regulated proteins in tumors. The proteins were categorized on the basis of GO annotation. The proportion of each category displayed is based on biological processes, cellular components, and molecular functions in percentage.

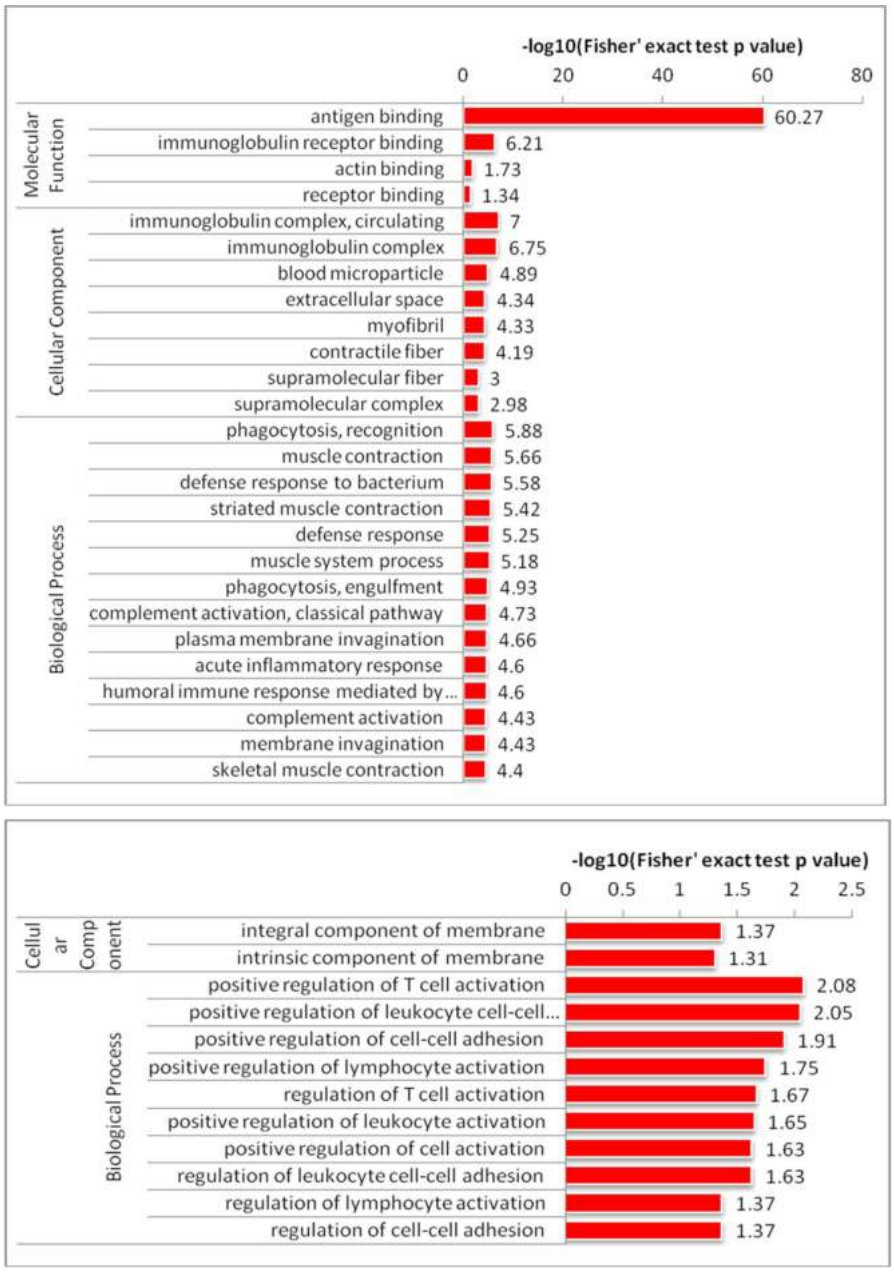

Fig. 4. GO secondary to ninth categories assigned to the significantly up (A) and down (B) regulated proteins in tumors. The proteins were categorized on the basis of GO annotation. The proportion of each category displayed is based on biological process, cellular component, and molecular function in –log 10 (Fisher's exact test p value).

second strongest inhibitory activity at a concentration of 0.5 mg/mL. The inhibitory activities of other samples tested were modest or weak.

There is a question about the discrepancies between the *in vitro* and *in vivo* studies. The major differences of the results between the *in vitro* and *in vivo* experiments are attributed to the interaction and the environment (Lorian, 1988). Samples interacted directly with A549 cells and the proteins in liquid media. However, samples may not interact directly with A549 cells and proteins in the *in vivo* experiments. Samples can indirectly exhibit activity through different pathways. The way in which samples are administered in the *in vivo* studies may make a difference to activity (Fitton, 2011). This is well illustrated in the research of Yanase and co-workers on the suppression of an IgE response to albumin by intraperitoneal fucoidan (Yanase et al., 2009). They found that fucoidan suppressed the stimulated increase of plasma IgE after being delivered intraperitoneally at 100 mcg per mouse, however, fucoidan did not suppress the stimulated increase of plasma IgE even after oral delivery at 10 mg per mouse. It is also interesting to note that fucoidan could reduce viral titres in mice after oral delivery (Hayashi, Hayashi, Kanekiyo, Ohta, & Lee, 2007). On the terms of the environment, cells were cultivated in artificial liquid media i*n vitro* experiments. However, in the *in vivo* experiments, A549 cells first must adhere, grow and proliferate in mice. The micorenvironment of A549 cells *in vivo* is totally different from that of A549 cells grown in artificial liquid media. And the microenvironment of A549 cells displays

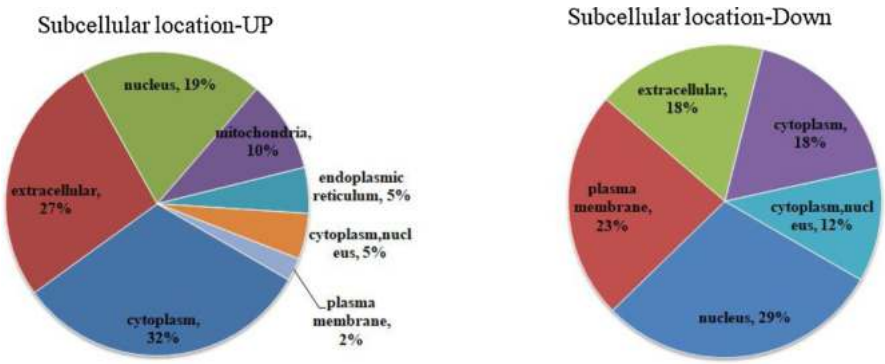

Fig. 5. Subcellular structure localization of the significantly up (A) and down (B) regulated proteins in tumors.

important roles in cancer initiation, progression and invasion (Lyssiotis & Kimmelman, 2017).

On the terms of structure-activity relationship of oligosaccharides and anti-tumor activity, several different types of oligosaccharides, including synthetic glycosides and degraded oligosaccharides, had been reported. In the anticancer activities of chitooligosaccharides with different degree of deacetylation, it was shown that a higher degree of deacetylation and lower molecular weights show the highest anticancer activity (Kim et al., 2012). For the anticancer activities of laminaran-oligosaccharides, it was shown that the lower molecular weights (degree of polymerization 9–23) with a higher content of 1,6-linked glucose residues had higher activity (Menshova et al., 2014). For the inhibitory activity of several synthetic sulfated mannooligosaccharides against heparanase, it was shown that the tetra- and penta-saccharides could totally inhibit heparanase while di- and trisaccharides did not completely inhibit heparanase even at very high concentrations (Fairweather, Hammond, Johnstone, & Ferro, 2008). In addition, pentasaccharide glycosides did not always have better activities than tetrasaccharide glycosides (Johnstone et al., 2010; Wall, Douglas, Ferro, Cowden, & Parish, 2001; Yu et al., 2002). Moreover, the growth inhibition on different types of cells, including leukemia, nonsmall cell lung cancer, colon cancer, melanoma, ovarian cancer, renal cancer, prostate cancer and breast cancer of tetrasaccharide glycosides were not always better than for trisaccharide glycosides (Shi et al., 2012; Sylla et al., 2014). It was interesting to note that trisaccharide glycosides also did not display greater anti-cancer activities than disaccharide glycosides (Wang et al., 2017). Finally, it was shown that the compounds with an α-configuration of terminal 2, 6-dideoxy sugar showed higher topoisomerase - poisoning than compounds with the β-configuration, indicating that sugar moieties in daunorubicin were important for anti-cancer activity and topoisomerase - inhibition (Zhang et al., 2005). In general, there was no absolute rule for the structure-activity relationship of oligosaccharides and anti-cancer activity.

5. Conclusion

Anti-lung cancer activities of glucuronomannan and its oligomers were carefully investigated in this study. Our data showed that G4 and G6 significantly inhibited the growth of A549 tumors. G6 exhibited the anti-lung cancer activity through the immune system based on its interaction with immunoglobulin. Our current study provides important insight into the application of oligosaccharides in the development of anti-lung cancer therapeutics.

CRediT authorship contribution statement

Weihua Jin: Conceptualization, Methodology, Data curation, Formal analysis, Funding acquisition, Resources, Writing - original draft, Supervision, Project administration. **Xinyue He:** Conceptualization, Methodology, Investigation, Formal analysis. **Jiachen Zhu:** Conceptualization, Methodology, Visualization. **Qiufu Fang:** Conceptualization, Methodology, Validation. **Bin Wei:** Methodology, Writing - review & editing. **Jiadong Sun:** Methodology, Writing - review & editing. **Wenjing Zhang:** Methodology, Writing - original draft, Writing - review & editing. **Zhongshan Zhang:** Methodology, Writing - review & editing. **Fuming Zhang:** Methodology, Writing - review & editing. **Robert J. Linhardt:** Writing - review & editing. **Hong Wang:** Writing - review & editing, Funding acquisition. **Weihong Zhong:** Writing - review & editing, Supervision.

Declaration of Competing Interest

The authors declare no conflicts of interest.

Acknowledgements

This study was supported by the National Key Research and Development Program of China (No. 2017YFE0103100); the National Natural Science Foundation of China (No. 41906095 and 41506165);

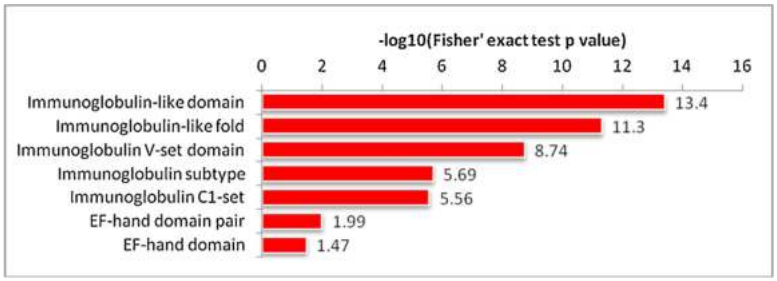

Fig. 6. Protein domain enrichment analysis of up regulated proteins.

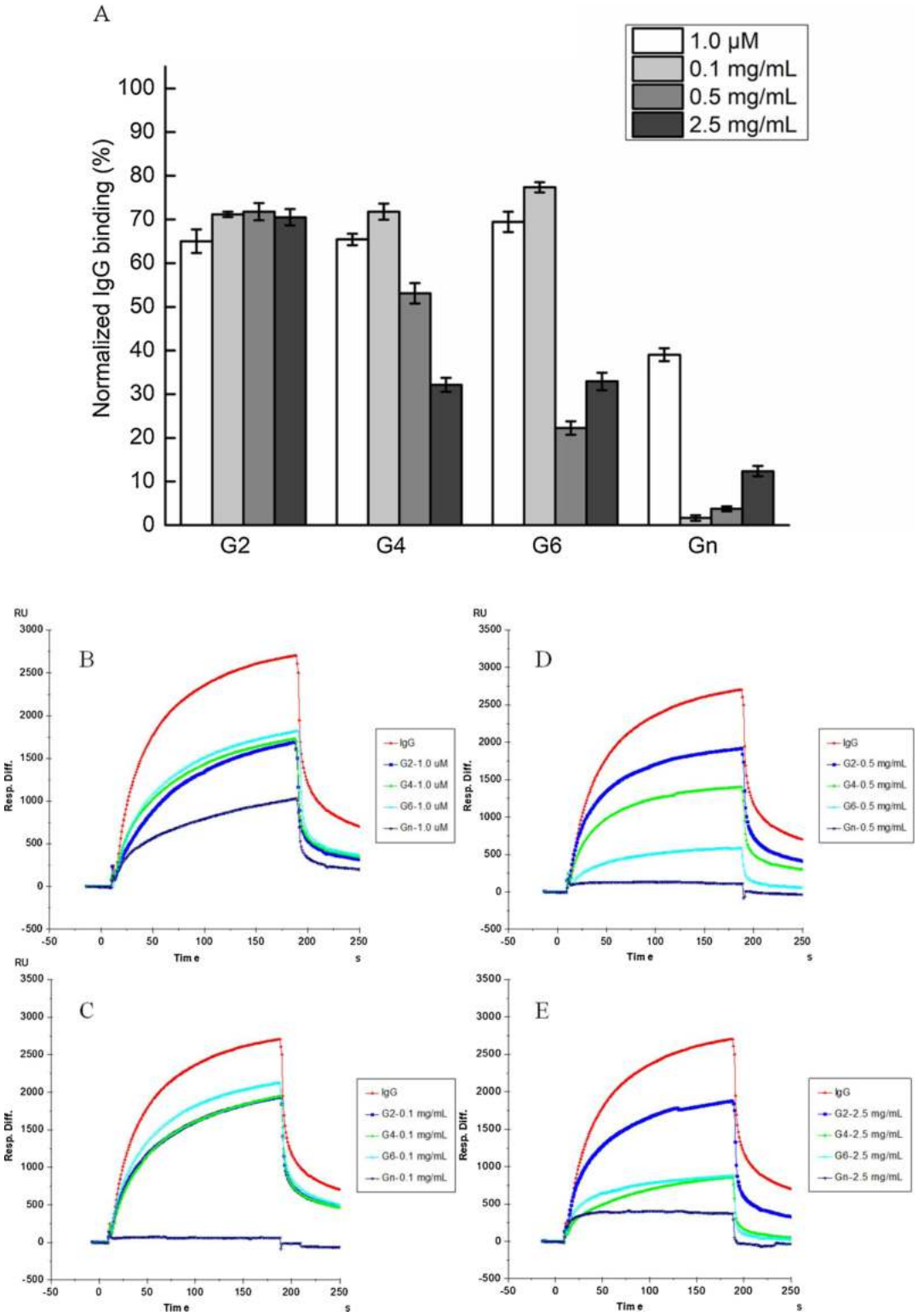

Fig. 7. SPR analysis of IgG binding. (A) Bar graphs and SPR sensorgrams of normalized IgG binding preference to surface heparin by competing with different concentrations of Gn and its oligomers (G2, G4 and G6). Concentrations were 1.0 μM (B), 0.1 mg/mL (C), 0.5 mg/mL (D) and 2.5 mg/mL (E), respectively. Data are presented as means ± SD of three independent experiments (n = 3).

the Zhejiang Provincial Natural Science Foundation of China (No. LY19D060006) and China Scholarship Council (W.J.).

Appendix A. Supplementary data

Supplementary material related to this article can be found, in the online version, at doi:https://doi.org/10.1016/j.carbpol.2020.116785.

References

Ackerman, D. L., Craft, K. M., Doster, R. S., Weitkamp, J. H., Aronoff, D. M., Gaddy, J. A., et al. (2018). Antimicrobial and antibiofilm activity of human milk oligosaccharides against *Streptococcus agalactiae*, *Staphylococcus aureus*, and *Acinetobacter baumannii*. *ACS Infectious Diseases, 4*(3), 315–324.

Agha-Mohammadi, S., & Lotze, M. T. (2000). Immunomodulation of cancer: Potential use of selectively replicating agents. *The Journal of Clinical Investigation, 105*(9), 1173–1176.

Ai, L., Chung, Y. C., Lin, S. Y., Jeng, K. G., Lai, P. F., Xiong, Z. Q., et al. (2018). Carrageenan polysaccharides and oligosaccharides with distinct immunomodulatory activities in murine microglia BV-2 cells. *International Journal of Biological Macromolecules, 120*(Pt A), 633–640.

Berteau, O., & Mulloy, B. (2003). Sulfated fucans, fresh perspectives: Structures, functions, and biological properties of sulfated fucans and an overview of enzymes active toward this class of polysaccharide. *Glycobiology, 13*(6) 29R-40R.

Chen, X., Nie, W., Yu, G., Li, Y., Hu, Y., Lu, J., et al. (2012). Antitumor and immunomodulatory activity of polysaccharides from *Sargassum fusiforme*. *Food and Chemical Toxicology, 50*(3–4), 695–700.

Cumashi, A., Ushakova, N. A., Preobrazhenskaya, M. E., D'Incecco, A., Piccoli, A., Totani, L., et al. (2007). A comparative study of the anti-inflammatory, anticoagulant, antiangiogenic, and antiadhesive activities of nine different fucoidans from brown seaweeds. *Glycobiology, 17*(5), 541–552.

Deniaud-Bouet, E., Hardouin, K., Potin, P., Kloareg, B., & Herve, C. (2017). A review about brown algal cell walls and fucose-containing sulfated polysaccharides: Cell wall context, biomedical properties and key research challenges. *Carbohydrate Polymers, 175*, 395–408.

Ehrrlich, P. (1999). Ueber den jetzigen stand der karzinoforschung. *Nederlands Tijdschrift Voor Geneeskunde, 5*, 273–290.

Fairweather, J. K., Hammond, E., Johnstone, K. D., & Ferro, V. (2008). Synthesis and heparanase inhibitory activity of sulfated mannooligosaccharides related to the antiangiogenic agent PI-88. *Bioorganic & Medicinal Chemistry, 16*(2), 699–709.

Fan, S., Yu, G., Nie, W., Jin, J., Chen, L., & Chen, X. (2018). Antitumor activity and underlying mechanism of *Sargassum fusiforme* polysaccharides in CNE-bearing mice. *International Journal of Biological Macromolecules, 112*, 516–522.

Feng, C., Ghosh, A., Amin, M. N., Bachvaroff, T. R., Tasumi, S., Pasek, M., et al. (2015). Galectin CvGal2 from the eastern oyster (*Crassostrea virginica*) displays unique specificity for ABH blood group oligosaccharides and differentially recognizes sympatric perkinsus species. *Biochemistry, 54*(30), 4711–4730.

Fitton, J. H. (2011). Therapies from fucoidan; multifunctional marine polymers. *Marine Drugs, 9*(10), 1731–1760.

Fitton, J. H., Stringer, D. N., & Karpiniec, S. S. (2015). Therapies from fucoidan: An update. *Marine Drugs, 13*(9), 5920–5946.

Garcia-Vaquero, M., Rajauria, G., O'Doherty, J. V., & Sweeney, T. (2017). Polysaccharides from macroalgae: Recent advances, innovative technologies and challenges in extraction and purification. *Food Research International, 99*(Pt 3), 1011–1020.

Gremski, L. A., Coelho, A. L. K., Santos, J. S., Daguer, H., Molognoni, L., do Prado-Silva, L., et al. (2019). Antioxidants-rich ice cream containing herbal extracts and fructooligossaccharides: manufacture, functional and sensory properties. *Food Chemistry, 298*, 125098.

Guan, G., Azad, M. A. K., Lin, Y., Kim, S. W., Tian, Y., Liu, G., et al. (2019). Biological effects and applications of chitosan and chito-oligosaccharides. *Frontier in Physiology, 10*, 516.

Hayashi, T., Hayashi, K., Kanekiyo, K., Ohta, Y., & Lee, J.-B. (2007). Promising antiviral glyco-molecules from an edible alga. In P. F. Torrence (Ed.). *Combating the threat of pandemic influenza: Drug discovery approaches* (pp. 166–182). Hoboken, NJ, USA: John Wiley & Sons.

Hsu, H. Y., & Hwang, P. A. (2019). Clinical applications of fucoidan in translational medicine for adjuvant cancer therapy. *Clinical and Translational Medicine, 8*(1), 15.

Jin, W., Ren, L., Liu, B., Zhang, Q., & Zhong, W. (2018). Structural features of sulfated glucuronomannan oligosaccharides and their antioxidant activity. *Marine Drugs, 16*(9).

Jin, W. H., Wang, J., Ren, S. M., Song, N., & Zhang, Q. B. (2012). Structural analysis of a heteropolysaccharide from *Saccharina japonica* by electrospray mass spectrometry in tandem with collision-induced dissociation tandem mass spectrometry (ESI-CID-MS/MS). *Marine Drugs, 10*(10), 2138–2152.

Johnstone, K. D., Karoli, T., Liu, L., Dredge, K., Copeman, E., Li, C. P., et al. (2010). Synthesis and biological evaluation of polysulfated oligosaccharide glycosides as inhibitors of angiogenesis and tumor growth. *Journal of Medicinal Chemistry, 53*(4), 1686–1699.

Khalil, D. N., Smith, E. L., Brentjens, R. J., & Wolchok, J. D. (2016). The future of cancer treatment: Immunomodulation, CARs and combination immunotherapy. *Nature Reviews Clinical Oncology, 13*(5), 273–290.

Kim, E. K., Je, J. Y., Lee, S. J., Kim, Y. S., Hwang, J. W., Sung, S. H., et al. (2012). Chitooligosaccharides induce apoptosis in human myeloid leukemia HL-60 cells. *Bioorganic & Medicinal Chemistry Letters, 22*(19), 6136–6138.

Kim, S. Y., Zhao, J., Liu, X., Fraser, K., Lin, L., Zhang, X., et al. (2017). Interaction of Zika virus envelope protein with glycosaminoglycans. *Biochemistry, 56*(8), 1151–1162.

Kusaykin, M., Bakunina, I., Sova, V., Ermakova, S., Kuznetsova, T., Besednova, N., et al. (2008). Structure, biological activity, and enzymatic transformation of fucoidans from the brown seaweeds. *Biotechnology Journal, 3*, 904–915.

Lang, Y., Zhao, X., Liu, L., & Yu, G. (2014). Applications of mass spectrometry to structural analysis of marine oligosaccharides. *Marine Drugs, 12*(7), 4005–4030.

Lee, Y. E., Kim, H., Seo, C., Park, T., Lee, K. B., Yoo, S. Y., et al. (2017). Marine polysaccharides: Therapeutic efficacy and biomedical applications. *Archives of Pharmacal Research, 40*(9), 1006–1020.

Li, B., Lu, F., Wei, X., & Zhao, R. (2008). Fucoidan: Structure and bioactivity. *Molecules, 13*, 1671–1695.

Li, Y. X., Yi, P., Liu, J., Yan, Q. J., & Jiang, Z. Q. (2018). High-level expression of an engineered beta-mannanase (mRmMan5A) in Pichia pastoris for manno-oligosaccharide production using steam explosion pretreated palm kernel cake. *Bioresource Technology, 256*, 30–37.

Lin, F., Yang, D., Huang, Y., Zhao, Y., Ye, J., & Xiao, M. (2019). The potential of neoagaro-oligosaccharides as a treatment of type II diabetes in mice. *Marine Drugs, 17*(10).

Liu, J., & Linhardt, R. J. (2014). Chemoenzymatic synthesis of heparan sulfate and heparin. *Nature Product Reports, 31*(12), 1676–1685.

Locy, H., de Mey, S., de Mey, W., De Ridder, M., Thielemans, K., & Maenhout, S. K. (2018). Immunomodulation of the tumor microenvironment: Turn foe into friend. *Frontiers in Immunology, 9*(2909).

Lorian, V. (1988). Differences between *in vitro* and *in vivo* studies. *Antimicrobial Agents and Chemotherapy, 32*(10), 1600–1601.

Luthuli, S., Wu, S., Cheng, Y., Zheng, X., Wu, M., & Tong, H. (2019). Therapeutic effects of fucoidan: A review on recent studies. *Marine Drugs, 17*(9).

Lyssiotis, C. A., & Kimmelman, A. C. (2017). Metabolic interactions in the tumor microenvironment. *Trends in Cell Biology, 27*(11), 863–875.

Matsushita, M., & Kawaguchi, M. (2018). Immunomodulatory effects of drugs for effective cancer immunotherapy. *International Journal of Oncology, 2018*, 8653489.

Mebius, R. E., & Kraal, G. (2005). Structure and function of the spleen. *Nature Reviews Immunology, 5*(8), 606–616.

Menshova, R. V., Ermakova, S. P., Anastyuk, S. D., Isakov, V. V., Dubrovskaya, Y. V., Kusaykin, M. I., et al. (2014). Structure, enzymatic transformation and anticancer activity of branched high molecular weight laminaran from brown alga *Eisenia bicyclis*. *Carbohydrate Polymers, 99*, 101–109.

Muanprasat, C., & Chatsudthipong, V. (2017). Chitosan oligosaccharide: Biological activities and potential therapeutic applications. *Pharmacology & Therapeutics, 170*, 80–97.

Pomin, V. H. (2010). Review: An overview about the structure-function relationship of marine sulfated homopolysaccharides with regular chemical structures. *Biopolymers, 93*(5) 496-496.

Pomin, V. H., & Mour˜ao, P. A. S. (2008). Structure, biology, evolution, and medical importance of sulfated fucans and galactans. *Glycobiology, 18*(12), 1016–1027.

Ray, C., Kerketta, J. A., Rao, S., Patel, S., Dutt, S., Arora, K., et al. (2019). Human milk oligosaccharides: The journey ahead. *International Journal of Pediatrics, 2019*, 2390240.

Sanjeewa, K. K. A., Lee, J. S., Kim, W. S., & Jeon, Y. J. (2017). The potential of brown-algae polysaccharides for the development of anticancer agents: An update on anticancer effects reported for fucoidan and laminaran. *Carbohydrate Polymers, 177*, 451–459.

Shi, P., Silva, M. C., Wang, H. Y., Wu, B., Akhmedov, N. G., Li, M., et al. (2012). Structure activity relationship study of the cleistriosides and cleistetrosides for antibacterial/anticancer activity. *ACS Medicinal Chemistry Letters, 3*(12), 1086–1090.

Sylla, B., Legentil, L., Saraswat-Ohri, S., Vashishta, A., Daniellou, R., Wang, H. W., et al. (2014). Oligo-beta-(1 – > 3)-glucans: impact of thio-bridges on immunostimulating activities and the development of cancer stem cells. *Journal of Medicinal Chemistry, 57*(20), 8280–8292.

Usov, A. I., & Bilan, M. I. (2009). Fucoidans-sulfatedd polysaccharides of brown algae. *Russian Chemical Reviews, 78*(8), 785–799.

Wall, D., Douglas, S., Ferro, V., Cowden, W., & Parish, C. (2001). Characterisation of the anticoagulant properties of a range of structurally diverse sulfated oligosaccharides. *Thrombosis Research, 103*(4), 325–335.

Wang, L., Wang, Z., Su, S., Xing, Y., Li, Y., Li, M., et al. (2017). Synthesis and cytotoxicity of oleanolic acid trisaccharide saponins. *Carbohydrate Research, 442*, 9–16.

Wang, P., Zhao, X., Lv, Y., Liu, Y., Lang, Y., Wu, J., et al. (2012). Analysis of structural heterogeneity of fucoidan from *Hizikia fusiforme* by ES-CID-MS/MS. *Carbohydrate Polymers, 90*(1), 602–607.

Wijesinghe, W. A. J. P., & Jeon, Y.-J. (2012). Biological activities and potential industrial applications of fucose rich sulfated polysaccharides and fucoidans isolated from brown seaweeds: A review. *Carbohydrate Polymers, 88*(1), 13–20.

Wilkowska, A., Nowak, A., Antczak-Chrobot, A., Motyl, I., Czyzowska, A., & Paliwoda, A. (2019). Structurally different pectic oligosaccharides produced from apple pomace and their biological activity *in vitro*. *Foods, 8*(9).

Wu, J., Lv, Y., Liu, X., Zhao, X., Jiao, G., Tai, W., et al. (2015). Structural study of sulfated fuco-oligosaccharide branched glucuronomannan from *Kjellmaniella crassifolia* by ESI-CID-MS/MS. *Journal of Carbohydrate Chemistry, 34*(5), 303–317.

Wu, L., Sun, J., Su, X., Yu, Q., Yu, Q., & Zhang, P. (2016). A review about the development of fucoidan in antitumor activity: Progress and challenges. *Carbohydrate Polymers, 154*, 96–111.

Xia, X., Zhu, L., Lei, Z., Song, Y., Tang, F., Yin, Z., et al. (2019). Feruloylated oligosaccharides alleviate dextran sulfate sodium-induced colitis in vivo. *Journal of Agriculture and Food Chemistry, 67*(34), 9522–9531.

Yadav, V. K., Mandal, R. S., Puniya, B. L., Kumar, R., Dey, S., Singh, S., et al. (2015).

Structural and binding studies of SAP-1 protein with heparin. *Chemical Biology & Drug Design, 85*(3), 404–410.

Yan, L., Wang, D., Zhu, M., Yu, Y., Zhang, F., Ye, X., et al. (2019). Highly purified fucosylated chondroitin sulfate oligomers with selective intrinsic factor Xase complex inhibition. *Carbohydrate Polymers, 222*, 115025.

Yanase, Y., Hiragun, T., Uchida, K., Ishii, K., Oomizu, S., Suzuki, H., et al. (2009). Peritoneal injection of fucoidan suppresses the increase of plasma IgE induced by OVA-sensitization. *Biochemical and Biophysical Research Communications, 387*(3), 435–439.

Young, I. D., Montilla, A., Olano, A., Wittmann, A., Kawasaki, N., & Villamiel, M. (2019). Effect of purification of galactooligosaccharides derived from lactulose with *Saccharomyces cerevisiae* on their capacity to bind immune cell receptor Dectin-2. *Food Research International, 115*, 10–15.

Yu, G., Gunay, N. S., Linhardt, R. J., Toida, T., Fareed, J., Hoppensteadt, D. A., et al. (2002). Preparation and anticoagulant activity of the phosphosulfomannan PI-88. *European Journal of Medicinal Chemistry, 37*(10), 783–791.

Yuan, X., Zheng, J., Jiao, S., Cheng, G., Feng, C., Du, Y., et al. (2019). A review on the preparation of chitosan oligosaccharides and application to human health, animal husbandry and agricultural production. *Carbohydrate Polymers, 220*, 60–70.

Zaporozhets, T., & Besednova, N. (2016). Prospects for the therapeutic application of sulfated polysaccharides of brown algae in diseases of the cardiovascular system: review. *Pharmaceutical Biology, 54*(12), 3126–3135.

Zhang, F., Lee, K. B., & Linhardt, R. J. (2015). SPR biosensor probing the interactions between TIMP-3 and heparin/GAGs. *Biosensors (Basel), 5*(3), 500–512.

Zhang, F., Moniz, H. A., Walcott, B., Moremen, K. W., Linhardt, R. J., & Wang, L. (2013). Characterization of the interaction between Robo1 and heparin and other glycosaminoglycans. *Biochimie, 95*(12), 2345–2353.

Zhang, G., Fang, L., Zhu, L., Aimiuwu, J. E., Shen, J., Cheng, H., et al. (2005). Syntheses and biological activities of disaccharide daunorubicins. *Journal of Medicinal Chemistry, 48*(16), 5269–5278.

Zhang, W., Yan, J., Wu, L., Yu, Y., Ye, R. D., Zhang, Y., et al. (2019). In vitro immunomodulatory effects of human milk oligosaccharides on murine macrophage RAW264.7 cells. *Carbohydrate Polymers, 207*, 230–238.

Zhang, F., Zheng, L., Cheng, S., Peng, Y., Fu, L., Zhang, X., et al. (2019). Comparison of the interactions of different growth factors and glycosaminoglycans. *Molecules, 24*(18).

Zhao, J., Huvent, I., Lippens, G., Eliezer, D., Zhang, A., Li, Q., et al. (2017). Glycan determinants of heparin-tau interaction. *Biophysical Journal, 112*(5), 921–932.